HOAPS precipitation validation with ship-borne rain gauge measurements over the Baltic Sea

By KARL BUMKE[1]*, KARSTEN FENNIG[2], ALEXANDER STREHZ[3], REBEKKA MECKING[1] and MARC SCHRÖDER[2], [1]Helmholtz-Zentrum für Ozeanforschung Kiel (GEOMAR), Düsternbrooker Weg 20, 24105 Kiel, Germany; [2]CM SAF, Deutscher Wetterdienst, Frankfurter Straße 135, 63067 Offenbach, Germany; [3]Department of Physics, University of Auckland, 5 Symonds Street, Auckland 1142, New Zealand

ABSTRACT

Global ocean precipitation is an important part of the water cycle in the climate system. A number of efforts have been undertaken to acquire reliable estimates of precipitation over the oceans based on remote sensing and reanalysis modelling. However, validation of these data is still a challenging task, mainly due to a lack of suitable in situ measurements of precipitation over the oceans. In this study, validation of the satellite-based Hamburg Ocean Atmosphere Parameters and fluxes from Satellite data (HOAPS) climatology was conducted with in situ measurements by ship rain gauges over the Baltic Sea from 1995 to 1997. The ship rain gauge data are point-to-area collocated against the HOAPS data. By choosing suitable collocation parameters, a detection rate of up to about 70% is achieved. Investigation of the influence of the synoptic situation on the detectability shows that HOAPS performs better for stratiform than for convective precipitation. The number of collocated data is not sufficient to validate precipitation rates. Thus, precipitation rates were analysed by applying an interpolation scheme based on the Kriging method to both data sets. It was found that HOAPS underestimates precipitation by about 10%, taking into account that precipitation rates below 0.3 mm h^{-1} cannot be detected from satellite information.

Keywords: Precipitation, ship rain gauge, satellite, validation, HOAPS

1. Introduction

A pre-requisite for understanding the global climate system is a good knowledge of the global water cycle (e.g. Chahine, 1992). However, measuring the required quantities especially over the oceans is still a challenging task. Aside from insufficient spatial and temporal coverage with ships or buoys, the main reason for a lack of available precipitation data can be attributed to the difficulty of measuring precipitation on moving platforms under high wind speeds.

The progress in satellite technology has provided the possibility to retrieve global data sets from space, including precipitation. Passive microwave radiometry allows for the estimation of several components of the water cycle. Levizzani et al. (2007) showed that precipitation over the oceans can be derived with sufficient accuracy from these data. On the other hand, Andersson et al. (2011) pointed out that even state-of-the-art satellite retrievals and reanalysis data sets still disagree on global precipitation with respect to amounts, patterns, variability and temporal behaviour, with the relative differences increasing in the pole-ward direction. This creates the need for ship-based precipitation validation data using instruments capable of accurately measuring rain rates even under high wind speed conditions.

In general, validation of remotely sensed precipitation data over sea is difficult since no comprehensive in situ data are available (Oki, 1999). Even for validation of upcoming satellite missions, it is planned to mainly use in situ measurements from island stations (e.g. Adkins et al., 2002), although instruments do exist, which are able to measure precipitation on ships with sufficient accuracy. One of these instruments is the ship rain gauge described by Hasse et al. (1998). A number of ship rain gauges had been mounted on merchant ships travelling from Germany to Finland over the Baltic Sea to estimate average precipitation rates for the Baltic Sea area (Clemens and Bumke,

*Corresponding author.
email: kbumke@geomar.de

1

2002). In this study, ship rain gauge data from 1995 to 1997 are used to yield a point-to-area collocation against the satellite-derived climatology Hamburg Ocean Atmosphere Parameters and fluxes from Satellite data (HOAPS; Andersson et al., 2010, 2011).

In general, there are two different approaches for comparing satellite data with in situ measurements. The in situ data can be interpolated to match the position of the satellite data or the satellite data is compared to the in situ measurement, which is closest (nearest neighbour).

In this study the second strategy was chosen, because interpolating data have some important disadvantages. To match satellite and in situ measurements via interpolation, the satellite measurement has to be surrounded by at least three in situ measurements, which are spatially and temporally close enough to avoid an impermissible extrapolation. This constraint reduces the number of data suitable for a collocation drastically. Another negative effect of interpolation is smoothing of data, for example, minima and maxima are reduced. Thus, the nearest neighbour approach was chosen. Therefore, it must be ensured that both observations are related to each other, which can be determined by the decorrelation length. The decorrelation length depends largely on the variable, climate zone and region considered. Precipitation itself has a very short decorrelation length in the mid-latitudes. Figure 1 shows the correlation functions of precipitation measurements over the Baltic Sea by an optical disdrometer (Großklaus et al., 1998) for 1-min intervals and for one hourly means. Corresponding decorrelation lengths are about 8 min and 2 h, respectively.

2. Shipboard and satellite precipitation data

2.1. Shipboard rain gauge

As mentioned above, satellite-based estimates of both frequency and amounts of precipitation have uncertainties. This calls for ground validation instruments capable of measuring shipboard precipitation under all weather conditions, including high sea-states, high relative wind speeds and irregular flow patterns around the ship's superstructure. Such an instrument is the ship rain gauge (Hasse et al., 1998), which is commercially available from Eigenbrodt Environmental Measurement Systems near Hamburg, Germany (Fig. 2).

An outstanding feature of the ship rain gauge is an additional lateral collector, which is effective especially under high wind speed conditions (Hasse et al., 1998). Collected water from the top and lateral collector in combination with measured wind speeds relative to the instrument allows the derivation of true rainfall rates. Therefore, the amount of rain has to be estimated
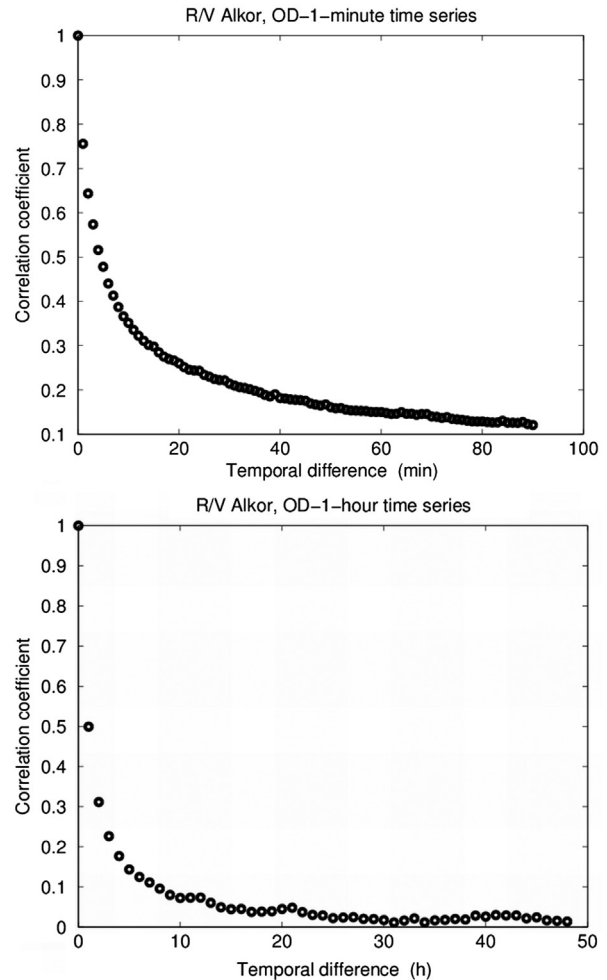

Fig. 1. Correlation functions for precipitation measurements derived from measurements using an optical disdrometer (Großklaus et al., 1998) on board of R/V Alkor over the Baltic Sea for 1-min averaging intervals (left) and hourly time series (right). Measurements are from 2000 until 2003.

separately for each collector. For low wind speeds, the catchment of the horizontal upper collector is quite accurate, and at high wind speeds measurements by the lateral collector obtain the least biased estimate of the rainfall. Finally, a wind speed-dependent algorithm is used to estimate the true rainfall rates. The algorithm includes a wind speed-dependent weighting between both collectors in the wind speed range from 9 to 11 ms^{-1}. Details of the algorithm are given in Clemens (2002). Comparisons to other instruments show that the ship rain gauge performs well and gives nearly unbiased estimates of rainfall (Clemens and Bumke, 2002).

In order to get the spatial distribution of rainfall over the Baltic Sea, several merchant ships (MS Translubeca, MS Transfinlandia, MS Antares, MS Railship I and MS

Railship 2) had been equipped with ship rain gauges. These ships travelled between Lübeck (Germany) and Helsinki (Finland) through the southern and central Baltic Sea. The instruments were installed onboard at sites where the flow is nearly horizontal. Relative wind speed measurements were taken from the same position; wind speeds are 8-min averages. Position and time at the end of each measurement interval were taken from GPS information. Rain measurements were stored at 8-min intervals. Measurements were randomly distributed in space and time along the shipping routes.

2.2. Satellite precipitation data

The satellite-derived HOAPS climatology is the only generally available compilation of both precipitation and evaporation data, with the goal of estimating the net freshwater flux from one consistently derived global satellite data set. To achieve this goal, HOAPS utilises multisatellite averages, inter-sensor calibration and an efficient sea ice detection procedure. All HOAPS variables are derived using radiances from the Special Sensor Microwave/Imager (SSM/I) radiometers, except for the sea surface temperature, which is obtained from the Advanced Very High Resolution Radiometer measurements (Andersson et al., 2010). Three data subsets of HOAPS-3 are available comprising scan-based pixel-level data (HOAPS-S) and two types of gridded data products (HOAPS-G and HOAPS-C), allowing HOAPS to be used for a wide range of applications. Compared to former

Fig. 2.   Sketch of the ship rain gauge showing the horizontal and lateral collectors and the drop forming devices.

versions, HOAPS-3 contains a completely reprocessed and extended time-series of global freshwater flux-related parameters. One key feature of the update is the introduction of a new precipitation algorithm (Andersson et al., 2010). The HOAPS-S data subset, used in the present study, contains all retrieved physical parameters at the native SSM/I pixel-level resolution of approximately 50 km for each individual satellite. The HOAPS-3 precipitation retrieval is based on a neural network utilising a training data set based on a one-dimensional variational retrieval that has been in operation at European Center for Medium-Range Weather Forecasts (ECMWF) between 2005 and 2009 (Andersson et al., 2010).

The detection of light rain is hampered by the sensitivity of the microwave imager. In the HOAPS precipitation algorithm, a precipitation signal below the threshold value is considered to be zero. From experience with the preceding HOAPS precipitation algorithm, a value of 0.3 mm h^{-1} turned out to be an appropriate limit for distinguishing between a real precipitation signal and background noise (Andersson et al., 2010). The algorithm does not discriminate between rain and snowfall. Due to the strong influence of increasing emissivity near land and sea ice covered areas, HOAPS is devoid of data within 50 km off any coastline or sea-ice. Therefore, ship data within the coastal zone is also neglected. All individual descending and ascending overpasses of the SSM/I radiometers are used for the ground validation. The position of the HOAPS data represents the centre of an instantaneous field of view.

3. Analyses of precipitation fields

To enable the comparison of average precipitation rates (Section 4.3), a procedure has been developed based on the Kriging method, as described by Bacchi and Kottegoda (1995) and Rubel (1996). In this study, a modified scheme is used to calculate the sampling error by a Monte Carlo generation (Clemens and Bumke, 2002). The procedure starts with the analysis of all existing in situ precipitation measurements and all HOAPS precipitation estimates over the Baltic Sea. They serve as input for estimating the sampling error, mean fields and spatial correlation functions on an 8-min timescale for measurements and 1-min timescale for HOAPS. The next steps are to obtain first-guess precipitation fields and spatial correlation functions on a seasonal time scale. The averaged fields based on the raw measurements or estimates, sampling variance estimates and spatial structural functions form the input for the main analysis procedure. The resulting gridded fields produced by Kriging are tuned to the estimated sampling variances and characterised by the interpolation error quantified by the so-called Kriging variance. Details of the method are given by Clemens and Bumke (2002).
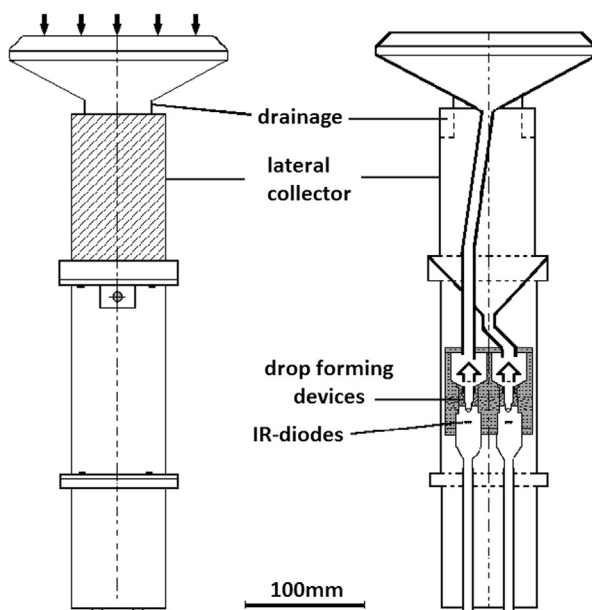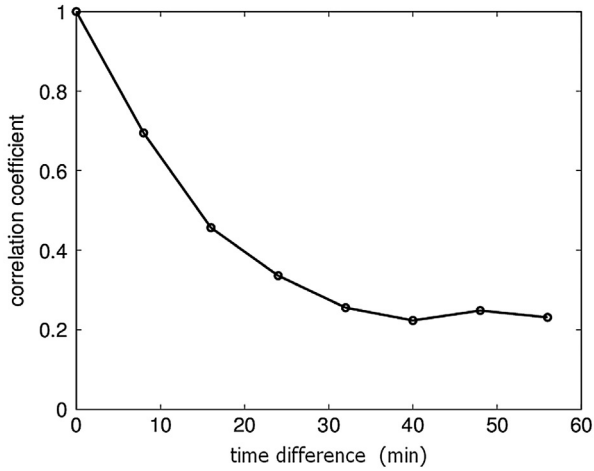
Fig. 3. Correlation function based on ship rain gauge measurements on merchant ships with 8-min integration time over the Baltic Sea area. Measurements are from 1995 until 1997.

4. Results

4.1. Detectability

For collocating data using the nearest neighbour approach, it is necessary to select reasonable temporal and spatial differences between in situ observations and satellite data. Hence, decorrelation lengths were derived from all available in situ precipitation data. Over the Baltic Sea, temporal and spatial decorrelation lengths based on the 8-min measurement intervals, assuming an average ship's speed of 20 kn, are 27 min and 17 km, respectively (Fig. 3). Therefore, the allowed time difference was set to 30 min and the allowed distance to 25 km, with regard to the spatial resolution of HOAPS (50 km).

These match-up criteria are a little stricter than the allowed differences of 45 min and 50 km chosen in a study by Klepp et al. (2010). The positions of the collocated data are limited to cases with a minimum measured precipitation rate of 0.3 mm h^{-1}, which are depicted in Fig. 4. For comparison, the figure indicates the locations of the satellites' footprints.

The following procedure has been chosen for validation. Collocated data have been merged to single events according to the time of the satellite overpass. Each event has been checked independently for the amount of precipitation, whether observations and satellite data detected precipitation. If one of the observations measured precipitation, the event was flagged as 'observed precipitation yes'; and if one of the satellite footprints gives precipitation, the event was flagged as 'HOAPS precipitation yes'. The only limitation was that measured precipitation rates of <0.01 mm h^{-1} were set to zero. Accordingly a measured precipitation rate of 0.01 mm h^{-1} is flagged as 'observed precipitation yes'.
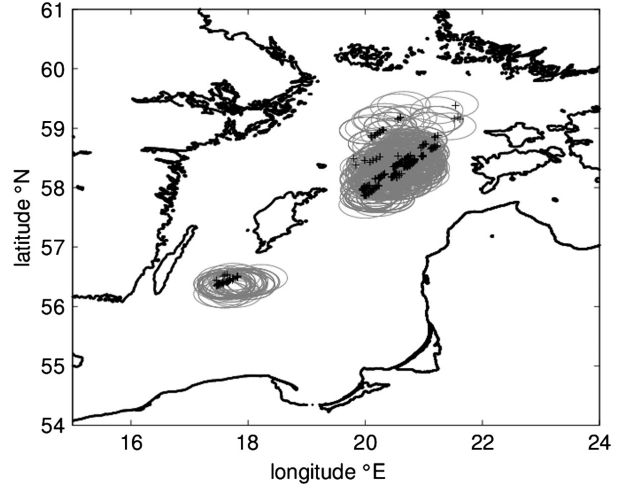

Fig. 4. Collocated ship measurements (black symbols) and HOAPS data. The HOAPS' footprints are indicated by the grey lines. Data are from 1995 until 1997, the minimum distance of the ships to the coast is 50 km.

The statistical analysis follows the recommendations given by the World Meteorological Organization (WMO) for binary or dichotomous forecasts (WWRP/WGNE: http://www.cawcr.gov.au/projects/verification/#Methods_for_dichotomous_forecasts). In the beginning a 2×2 contingency table is computed from the data, as shown in Table 1. These frequencies of 'yes' and 'no' HOAPS data and corresponding observations give a proportion correct of 0.90 for all 1395 events, which seems to be quite good. Since the Hansen–Kuipers Skill Score and the probability of detection have the same values, we have to take into account that precipitation has to be regarded as a rare event. In this case, a better estimate of the performance is the so-called threat score or critical success index (CSI) instead of the proportion correct. The CSI is 0.34 for the collocated data. Since there are no cases of HOAPS precipitation 'yes' when observed precipitation is 'no',

Table 1. 2×2 contingency table for measured precipitation ≥ 0.01 mm h^{-1} and HOAPS precipitation ≥ 0.3 mm h^{-1}. Collocated data have been merged to single events according to the time of the satellite's overpass

HOAPS precipitation (≥ 0.3 mm h^{-1})	Measured precipitation ≥ 0.01 mm h^{-1}		
	Yes	No	Total
Yes	71	0	71
No	136	1188	1324
Total	207	1188	1395

this number multiplied by 100 gives the detectability of observed precipitation by HOAPS in per cent. In other words, only 34% of events with measured rain are detected by HOAPS. In fact this number is misleading, since HOAPS data does not give precipitation rates of <0.3 mm h^{-1} due to limitations of the signal to noise ratio. Thus, with respect to the fact that HOAPS gives an areal estimate and ship measurements represent more point measurements, the lower limit of the observed precipitation rate should also be set to 0.3 mm h^{-1}. This reduces the number of events with observed precipitation to 83 over the Baltic Sea. The number of detected observed precipitation increases to 55% based on the corresponding contingency table, which is given in Table 2.

To test the dependency between the detection rate of observed precipitation and the lower limit of observed precipitation rate, the allowed temporal and spatial distances for collocation have been increased to 45 min and 50 km to increase the number of available events of collocated data. These limits agree with those of a study by Klepp et al. (2010). The results are given in Fig. 5. The figure depicts that the degree of detected observed precipitation increases up to about 70% with an increasing lower limit of observed precipitation rates, and changes become small for precipitation rates above 0.5 mm h^{-1}. The number of collocated events decreases from 414 at 0.01 mm h^{-1} to 44 at 2 mm h^{-1} measured precipitation rate.

Collocated data may also be used to investigate, whether the chosen temporal and spatial window for collocating satellite data and observations is reasonable. This has been tested by increasing the allowed temporal differences to 2 h and the spatial difference to 100 km in maximum for collocation. The resulting pairs of collocated data were used to estimate the detection rate of precipitation as a function of the time difference and spatial distance between observation and satellite data. In contrast to above, all single pairs of collocated data have been used, that is, data have not been merged to events. Figure 6 gives the results as a function of the time difference. Therefore, the allowed

Table 2. 2 × 2 contingency table for measured precipitation and HOAPS precipitation, both ≥ 0.3 mm h^{-1}. Collocated data have been merged to single events according to the time of the satellite's overpass

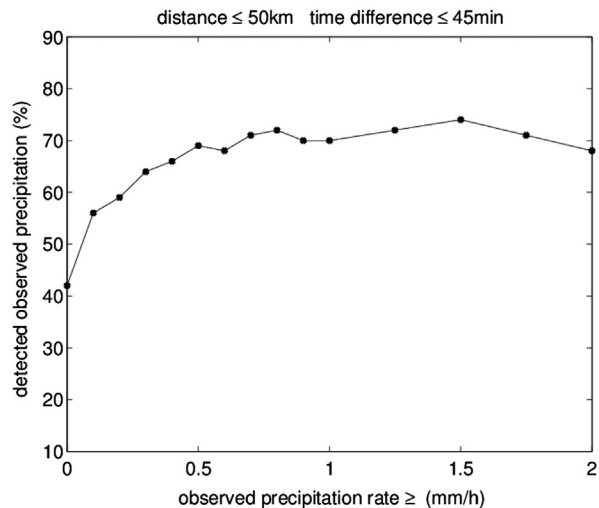| HOAPS precipitation	Measured precipitation ≥ 0.3 mm h^{-1}		
	Yes	No	Total
Yes	46	0	46
No	37	1312	1352
Total	83	1312	1395

Fig. 5. Detection of observed precipitation as a function of observed precipitation rate for collocated precipitation measurements and HOAPS data. Allowed temporal distance for collocation is 45 minutes, and the allowed spatial distance is 50 km.

spatial distance between observation and satellite has been set constant at 15 km and the lower limit in observed precipitation to 0.5 mm h^{-1}. Then, detection rates were calculated for time windows of 5-min width. Since detection rates show a considerable variation, a running mean has been computed for 11-min intervals. The calculated detection rate is nearly constant up to a time difference between observations and the satellites' overpass of about
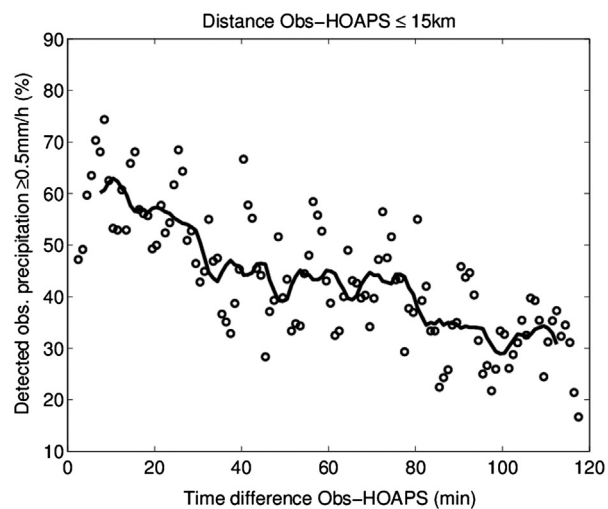

Fig. 6. Detected observed precipitation as a function of the time difference between observation and HOAPS data. The distance between measurement and HOAPS data is less than or equal to 15 km, the minimum of measured precipitation rate is 0.5 mm h^{-1}. The full line gives the running mean over 11 minutes.
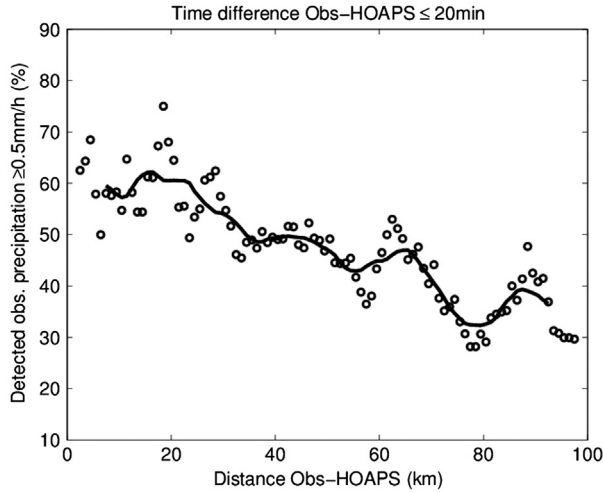
Fig. 7. Detected observed precipitation as a function of the distance between observation and HOAPS data. Time difference is less than or equal to 20 minutes, the minimum of measured precipitation rate is 0.5 mm h^{-1}. The full line gives a running mean over 11 km.

30 min. This agrees well with the decorrelation length of 27 min estimated from in situ observations (Fig. 3).

The results as a function of the spatial distance between observation and satellite's footprint are given in Fig. 7. Here, the spatial window has a width of 5 km, the allowed time difference between observation time and satellite overpasses is set constant to 20 minutes and the lower limit in observed precipitation is again 0.5 mm h^{-1}. As before, a running mean, now for 11-km intervals, has been calculated.

Figure 7 shows nearly constant detection rates up to a distance of about 25 km, which is also in acceptable agreement with the estimated decorrelation length of 17 km from in situ observations.

4.2. Detectability and the synoptic situation

From studies about the beamfilling error (e.g. Kummerow, 1996) one may expect that the synoptic situation influences the detectability of precipitation for satellite-based measurements. The idea is that the detection of small-scale convective precipitation events is more difficult than of stratiform precipitation due to the spatial extent of the SSM/I footprints. To investigate this, information from weather maps (Deutscher Wetterdienst, 1995, 1996, 1997), forecasts of the former Europamodell of the DWD (German Weather Service) (Majewski, 1991) and infrared satellite pictures (Dundee Satellite Receiving Station, 1995–1997) have been used.

Cloud types have been estimated visually from satellite images for all events, where precipitation had been measured. These events were divided into three categories: precipitation from stratiform clouds, from convective clouds and from clouds where the prevailing cloud type is uncertain. For each category the detectability was computed separately, with results given in Table 3. The detectability was calculated for a minimum in measured precipitation of 0.3 mm h^{-1}.

The results show that the detectability of precipitation from stratiform clouds is much better than from convective clouds.

The degree of cloudiness has been taken from 6- to 24-h forecasts of the Europamodell of the DWD to characterise the atmospheric conditions. Full cloudiness was taken as an indicator for the presence of large-scale stratiform clouds, while a partly cloudiness represents convective clouds. A more or less cloud-free sky also indicates the presence of single convective clouds. These results are given in Table 4 and again depict that under stratiform conditions the detectability is much better than under convective conditions.

Since the prevailing stratiform and convective clouds are characteristic for synoptical frontal systems, weather maps have been studied with respect to the occurrence of such fronts in the presence of measured precipitation. Only in seven cases of measured precipitation, no front was found in the weather maps; in all other cases warm fronts, cold fronts or occlusions could be detected. The results of the detectability of measured precipitation by HOAPS in the presence of different fronts are given in Table 5. It was found that precipitation in connection with warm fronts and occlusions could be detected much better than in the presence of cold fronts or away from any front. Under the assumption that stratiform clouds or extended areas of cloudiness are typical for warm fronts or occlusions, this supports the result that the detectability of precipitation from stratiform clouds by HOAPS is much better than under convective conditions. In fact this is not surprising since the horizontal extent of convective precipitating clouds is typically much smaller than the area of a satellite footprint. Therefore, precipitation can be measured on a ship, whereas the satellite gives no precipitation for the footprint area due to the cut-off at 0.3 mm h^{-1}.

Table 3. Measurements of precipitation and their detectability by HOAPS as a function of the cloud type as it was estimated from infrared satellite images

Cloud type	Stratiform	Cloud free and convective	No prevailing cloud type
Number measured	42	22	19
Number HOAPS	34	3	9
Detectability (%)	81	14	47

Table 4. Measurements of precipitation and their detectability by HOAPS as a function of the degree of cloudiness. The cloudiness was taken from the 6- to 24-h weather forecasts of the Europamodell, interpolated linearly in space and time to the ship measurements

Cloudiness	More or less cloud free	Sky is overcast	Partly cloudy
Number measured	5	47	31
Number HOAPS	0	34	12
Detectability (%)	0	60	39

4.3. Average precipitation rates

Although the number of observations is not sufficient to directly compare precipitation rates given by HOAPS and by observations, one might compare the average precipitation rates. For a time window of 30 min and a spatial window of 25 km for collocation, there are at least 1591 events. The probability of precipitation is 15% based on observed precipitation. Taking only precipitation observations of $0.3 \, \mathrm{mm \, h^{-1}}$ and more into account, the probability decreases to only 6%. Satellite data show a precipitation probability of 5%. The mean precipitation rate is $0.074 \, \mathrm{mm \, h^{-1}}$ for the in situ observations and $0.051 \, \mathrm{mm \, h^{-1}}$ for HOAPS data, which is about 30% lower than the measured precipitation rate. Based on all ship observations, it can be estimated that 10% of the difference can be explained by events having an observed precipitation rate of $<0.3 \, \mathrm{mm \, h^{-1}}$. The remaining difference of 20% is much bigger than known uncertainties of ship rain gauge measurements (Clemens and Bumke, 2002) and might be caused by uncertainties in the algorithm computing precipitation from SSM/I satellites or due to differences in data coverage.

To better understand if HOAPS really underestimates precipitation over the Baltic Sea, average precipitation rates were estimated from all available measurements and all available HOAPS data over the open Baltic Sea by applying an interpolation scheme based on the Kriging method, as briefly described in Section 3.

Table 5. Measurements of precipitation and their detectability by HOAPS as a function of the type of fronts as estimated from weather maps (Deutscher Wetterdienst, 1995, 1996, 1997) close to locations of measured precipitation

Type of front	No front	Cold front	Warm front	Occlusion
Number measured	20	24	7	32
Number HOAPS	7	6	7	26
Detectability (%)	35	25	100	81

The amount of data allows a calculation of average precipitation rates for the Baltic Sea in 1996 and 1997 on the regular grid of the Europamodell of the DWD with a resolution of approximately 0.5 degrees in latitude and longitude. Taking only grid points into account, where we have simultaneous estimates from satellite data and ship measurements, we acquire an average annual precipitation of 500 mm in 1996 and 400 mm in 1997 for HOAPS and 549 mm in 1996 and 564 mm in 1997 for ship measurements (Fig. 8). The underestimation of precipitation is obviously higher in 1996 than in 1997, summarised for both years it is on the order of 20%. Taking again into consideration that precipitation rates of $<0.3 \, \mathrm{mm \, h^{-1}}$ account for approximately 10% of all precipitation over the Baltic Sea, as it was estimated from all ship observations, the resuming underestimation of precipitation by HOAPS is about 10% for the central Baltic Sea area. The numbers have to be seen in the context of the interpolation error quantified by the so-called Kriging variance, which is on the order of 15% for interpolated fields from ship measurements and about 30% for interpolated fields based on the HOAPS data set indicating the paucity in satellite data.

5. Conclusions

Three years of data of in situ precipitation measurements over the Baltic Sea were used to investigate whether it is possible to validate remotely sensed precipitation estimates over sea.

Several conclusions can be drawn from this study. First, this study has clearly shown that the main problems for validating satellite-derived precipitation over sea are on one hand the paucity of satellite data and the available number of ship observations, while on the other hand the fact that precipitation, even in an area within the mid-latitudes, is a rare event, as clearly depicted by above statistics.

Nevertheless, results show that it is possible to estimate the detectability of measured precipitation by remote sensing, in this case HOAPS. Detectability of measured precipitation by HOAPS reaches values up to about 70%, depending on rain rate. Looking more into detail it was shown that the synoptic situation strongly influences the detectability. In cases of small-scale precipitation as typical for convective conditions, detectability goes down to values of $<50\%$. In the presence of prevailing stratiform clouds, detectability reaches values up to 100%.

Unfortunately the number of collocated observations is not sufficient to compare precipitation rates directly. Therefore, it is necessary to use an interpolation scheme, for example a scheme based on Kriging, as it was applied in this study. The resulting underestimation of HOAPS is on the order of 20% for 1996 and 1997. However, it has to be taken into account that, as estimated from ship observa-
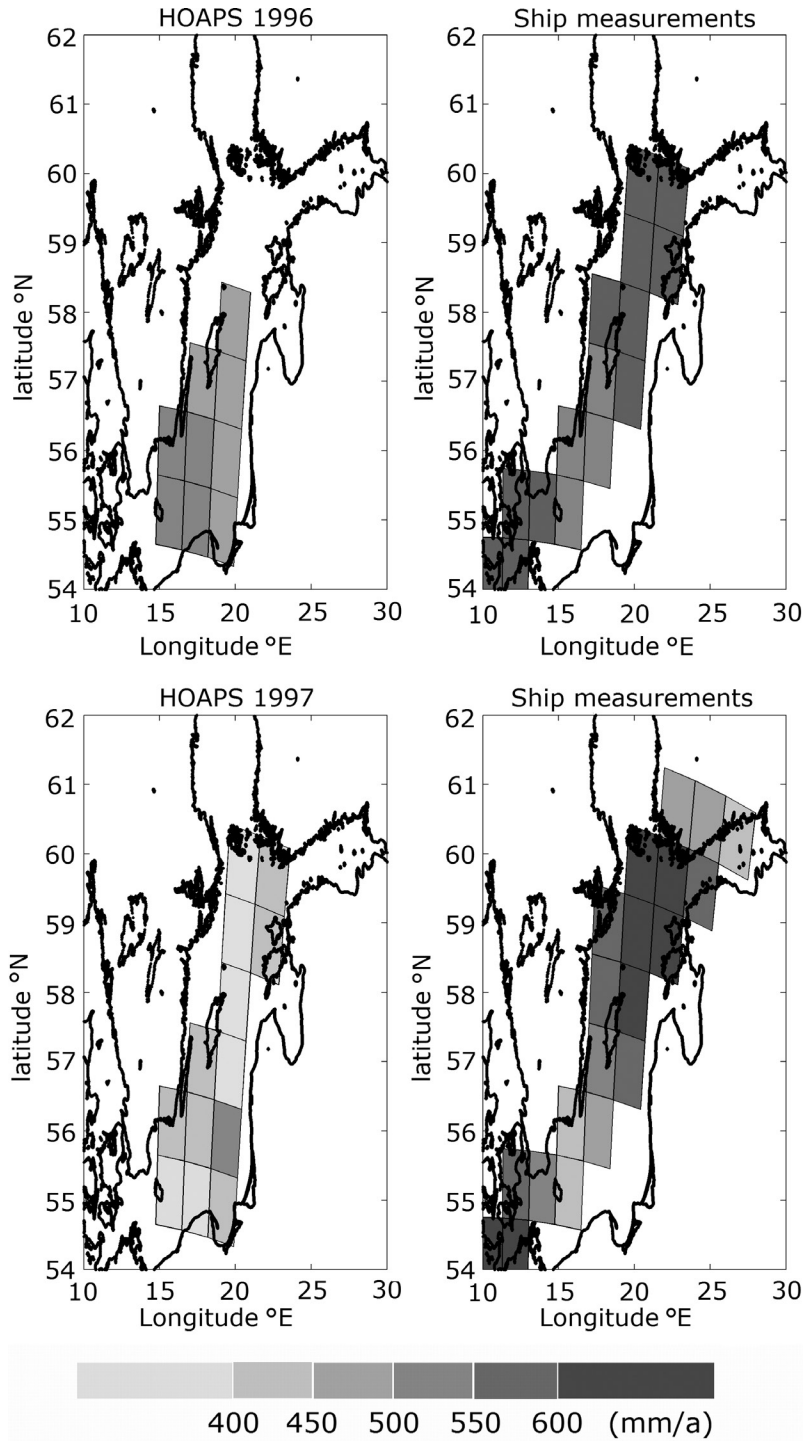
Fig. 8.   Analysed precipitation rates over the Baltic Sea based on HOAPS (left) and ship rain gauge measurements (right) for 1996 (top) and 1997 (bottom). Results are from an analysis based on the Kriging method (Clemens, 2002).

tions, precipitation rates of <0.3 mm h^{-1} account for 10% of the precipitation sum on average. Thus, one can state that HOAPS underestimates precipitation by at least 10% over the Baltic Sea.

The interpolation scheme also gives an estimate about the interpolation error for the calculated precipitation fields. The uncertainties in interpolated satellite data are about a factor of two higher than for interpolated fields

based on ship observations, also indicating the paucity in available satellite data.

Thus, improvements of the validation are possible by increasing the number of years included in the comparisons to put the statistics on a broader database. It is planned to use ship rain gauge data over the Baltic from later years as well as to extend comparisons to data available from research vessels.

It should be noted that this is only one step with respect to a successful understanding and modelling of the global climate system. Therefore, not only a thorough knowledge of the global ocean precipitation is required, but also information of evaporation to complete the water budget at the air sea interface is required, which is an important input for modelling of oceanic currents. Such data are part of HOAPS. Unfortunately, validation of evaporation is also hampered by the number of available ship measurements of evaporation (e.g. Large and Yeager, 2009).

References

Adkins, W., Yuter, S., Smith, E. A. and Adams, W. J. 2002. *Global Precipitation Measurement – Report* 5. Potential Tropical Open Ocean Precipitation Validation Sites, NASA/TM – 2002-210010, 78 p.

Andersson, A., Fennig, K., Klepp, C., Bakan, S., Graßl, H. and co-authors. 2010. The Hamburg Ocean Atmosphere Parameters and Fluxes from Satellite Data – HOAPS-3. *Earth Syst. Sci. Data* 2, 215–234, doi:10.5194/essd-2-215-2010.

Andersson, A., Klepp, C., Fennig, K., Bakan, S., Graßl, H. and co-authors. 2011. Evaluation of HOAPS-3 ocean surface freshwater flux components. *J. Appl. Meteorol. Climatol.* **50**, 379–398, doi:10.1175/2010JAMC2341.1.

Bacchi, B. and Kottegoda, N. T. 1995. Identification and calibration of spatial correlation patterns of rainfall. *J. Hydrol.* **165**, 311–348.

Chahine, M. T. 1992. The hydrological cycle and its influence on climate. *Nature* **359**, 373–380.

Clemens, M. 2002. *Machbarkeitsstudie zur räumlichen Niederschlagsanalyse aus Schiffsmessungen über der Ostsee*. Dissertation. Institut für Meereskunde an der Christian-Albrechts-Universität Kiel.

Clemens, M. and Bumke, K. 2002. Precipitation fields over the Baltic Sea derived from ship rain gauge measurements on merchant ships. *Boreal Environ. Res.* **7**, 425–436.

Deutscher Wetterdienst. 1995. *Europäischer Wetterbericht*, Vol. 20, No 1–365, Deutscher Wetterdienst, Offenbach.

Deutscher Wetterdienst. 1996. *Europäischer Wetterbericht*, Vol. 21, No 1–366, Deutscher Wetterdienst, Offenbach.

Deutscher Wetterdienst. 1997. *Europäischer Wetterbericht*, Vol. 22, No 1–365, Deutscher Wetterdienst, Offenbach.

Dundee Satellite Receiving Station. 1995–1997. Satellite pictures (thermal, infra-red, 10.3–11.3 μm), Online at: http://www.sat.dundee.ac.uk

Großklaus, M., Uhlig, K. and Hasse, L. 1998. An optical disdrometer for use in high wind speeds. *J. Atmos. Oceanic Technol.* **15**, 1051–1059.

Hasse, L., Großklaus, M., Uhlig, K. and Timm, P. 1998. A ship rain gauge for use under high wind speeds. *J. Atmos. Oceanic Technol.* **15**, 380–386.

Klepp, C., Bumke, K., Bakan, S. and Bauer, P. 2010. Ground validation of oceanic snowfall detection in satellite climatologies during LOFZY. *Tellus Series A: Dynamic Meteorology and Oceanography* **62**(4), 469–480. doi: 10.1111/j.1600-0870.2010.00459.x.

Kummerow, C. 1998. Beamfilling errors in passive microwave rainfall retrievals. *J. Appl. Meteorol.* **37**, 356–370.

Large, W. G. and Yeager, S. G. 2009. The global climatology of an interannually varying air-sea flux data set. *Clim. Dynamics* **33**, 341–364.

Levizzani, V., Bauer, P. and Turk, F. J. (eds.) 2007. *Measuring Precipitation from Space, EURAINSAT and the Future. Advances in Global Change Research*, Vol. 28, Springer, Dordrecht, Netherlands, 724 p.

Majewski, D. 1991. The Europa-Modell of the Deutscher Wetterdienst. *Seminar proceedings ECMWF* **2**, 147–191.

Oki, T. 1999. The global water cycle. In: *Global Energy and Water Cycles* (eds. K. A. Browning and R. J. Gurney) Cambridge University Press, Cambridge, pp. 10–29.

Rubel, F. 1996. PIDCAP-quick look precipitation atlas. *Österreichische Beiträge zu Meteorologie und Geophysik* **15**, Institute for Meteorology and Geophysics, University of Vienna, 95 pp.

WWRP/WGNE. 2012. Methods for dichotomous forecasts. Online at: www.cawcr.gov.au/projects/verification/#Methods_for_dichotomous_forecasts, Joint Working Group on Verification sponsored by the WMO, forecast verification, issues, methods and FAQ.